Finite-Element Panel Flutter in Three-Dimensional Supersonic Unsteady Potential Flow

T. Y. Yang* and S. H. Sung†
Purdue University, West Lafayette, Ind.

A finite-element formulation and solution procedure are developed for flutter prediction of rectangular panels with one surface exposed to three-dimensional supersonic unsteady potential flow. Each element is divided into several Mach boxes. The aerodynamic influence coefficients between each pair of sending and receiving boxes are computed by the method of Gaussian quadrature. The aerodynamic matrix is based on the numerically computed velocity potentials for all boxes. The effect of in-plane force is included. This development is particularly useful in the low supersonic range for panels with chord-span ratio less than about one, where the piston theory does not give satisfactory accuracy. Examples are demonstrated by using the 16 d.o.f. rectangular plate element. Results for flutter boundaries for the unstressed panels agree well with an alternative Galerkin's modal solution. The examples demonstrate that flutter boundaries are dominated by higher modes for panels with higher chord-span ratio. They also demonstrate that the dominating flutter boundaries abruptly change modes as the Mach number is varied. The beneficial effect of in-plane tension is demonstrated.

Nomenclature

a,b	= length and width of the rectangular plate finite element as defined in Fig. 1
B_x, B_{xs}	= number of boxes in the stream and cross-stream directions, respectively
D	$= Eh^3/12(1-\nu^2)$, bending rigidity
F	$= N_x/\ell^2\omega_1^2\sigma h$, Initial in-plane tension parameter
$f_j(x,y)$	= shape function associated with d.o.f. j
g	= structural damping coefficient
h	= panel thickness
i,j	= subscripts indicating d.o.f. number
k_ℓ, k_ϵ	$= \omega\ell/V$, $\omega\epsilon/V$, respectively, reduced frequency
ℓ	= length of panel in stream direction
M	= Mach number
m,n	= receiving box index numbers in the stream and cross-stream directions, respectively
N_x, N_y, N_{xy}	= panel in-plane line forces
r,s	$= (m-\lambda)$, $(n-\nu)$, respectively
u,v	= transformed variables of integration based on $\epsilon/2$ as reference length, $u\beta/2 = x_m - \xi$, $v/2 = y_n - \eta$
V	= speed of undisturbed airstream
w	= width of panel in cross-stream direction
w_j	= downwash velocity at panel surface for d.o.f. j
x,y	= panel coordinates as defined in Fig. 1
$\bar{x},\bar{y}$	$= x/\ell$, y/w, respectively
x_m, y_n	= values of x/ϵ and y/ϵ at center of box m,n
α_ϕ	= aerodynamic influence coefficient relating the velocity potential at a box to unit downswash on another box [Eq. (12)]
β	$= (M^2-1)^{1/2}$
ϵ	$= w/B_{xs}$, box width
ξ,η	= values of x/ϵ and y/ϵ at any point in the sending box
μ	= panel-air mass density ratio, $\sigma h/\rho\ell$
λ,ν	= sending box index number in the stream and cross-stream directions, respectively
ρ	= density of undisturbed airstream
σ	= density of panel
τ	= length-width ratio of box as defined in Fig. 1
$\phi_j(m,n)$	= velocity potential at center of box m,n for d.o.f. j
$\bar{\phi}(m,n)$	= velocity potential at center of box m,n due to unit downwash over box λ,ν
ω	= frequency of flutter motion
ω_1	= first natural frequency of the panel
Ω	$= (\omega_1/\omega)^2(1+ig)$
$\bar{\Omega}$	$= M^2 k_\epsilon/\beta^2$

Received Oct. 20, 1976; revision received Aug. 4, 1977.
Index categories: Aeroelasticity and Hydroelasticity; Structural Dynamics; Supersonic and Hypersonic Flow.

*Professor, School of Aeronautics and Astronautics. Associate Fellow AIAA.
†Amelia Earhart Fellow. Now at Fluid Dynamics Research Department, General Motors Research Lab.

Introduction

EVER since the earliest days of manned flight, panel flutter has been known as one of the most important problems in the design of aircrafts, missles, launched vehicles, and spacecrafts. Extensive progress in flutter tests and theoretical studies has been achieved. The basic theories and an account of the developments on panel flutter can be found in, among other books, a recent text by Dowell.[1] A list of keyed bibliography and collection of some significant survey papers and original papers was prepared by Garrick.[2]

In the theoretical analysis, it is essential that appropriate aerodynamic and structural theories are used. One of the most common formulation procedures is based on the modal superposition concept. In this method, a set of natural frequencies and normal mode shapes for the panel structure is first found. Based on the superposition of a sufficient number of such modes, the aerodynamic pressure and the inertial and elastic forces of the panel are obtained. The natural frequencies and modes can be found either by measurement or computation, or both. Among the computational methods, the finite-element method is gaining widespread acceptance because of its flexibility in handling the geometry and boundary conditions and the increasing accessibility of such computer codes.

As an alternative approach, finite-element workers have studied the formulation of the matrix of aeroydnamic pressure by using the displacement functions as composed of the nodal degrees of freedom and shape functions rather than the generalized coordinates and natural mode shapes. Such an approach can solve directly for the flutter frequencies and corresponding normal mode shapes without having to seek the natural frequencies and modes and choose the number of modes before the eigensolution, and also without having to compute the flutter mode shapes after the eigen-

solution. Such an approach permits expression of the equations of motion in a straightforward form. Such an approach also permits generality in panel configurations and boundary conditions, and allows one to include accurately physical effects such as in-plane forces.

The finite-element method was first extended to panel flutter problems by Olson.[3] He formulated the aerodynamic matrix explicitly for an infinite plate element. Olson[4] later formulated the aerodynamic matrices for two rectangular [12 and 16 degree-of-freedom (d.o.f)] and an 18 d.o.f. triangular plate elements. Simultaneously but independently, Appa and Somashekar[5] formulated the aerodynamic matrix for a 12 d.o.f. rectangular plate element. Appa et al.[6] later extended their work by accounting for skew panels and yawed flow by means of coordinate transformation. Sander et al.[7] employed the CQ conforming quadrilateral plate finite element for flutter analysis of rectangular panels with yawed flow and in-plane stresses.

In all of the preceding finite-element works,[3-7] Lighthill's linearized piston theory was employed. The Mach numbers considered were above approximately 1.6. Recently, Yang[8] developed a finite-element procedure using the exact linearized two-dimensional theory (strip theory) for unsteady supersonic flow to formulate an infinite plate finite element by means of numerical integration. Thus, the flutter speed considered could be in the lower supersonic range. Such a formulation, however, cannot be applied to the more general case of rectangular panels with finite aspect ratios. In order to account for the effects of finite aspect ratio and low supersonic speed, it appears necessary to use the three-dimensional supersonic unsteady potential flow theory.

The three-dimensional supersonic potential flow theory was employed by Appa[9] in formulating the aerodynamic influence coefficients relating grid points. The method was applied to a delta panel using triangular gridworks, and good results were obtained for steady and unsteady lift and moment coefficients. The degrees of freedom treated were, however, limited to linear displacement only. Such elements cannot be directly used with the triangular plate finite elements in panel flutter analysis for two reasons: 1) the elements do not have the first and second displacement derivative degrees of freedom, such as those contained in the common plate finite elements; and 2) for an accurate panel flutter analysis, the required number of plate finite elements is far less than that of the aerodynamic boxes. Thus, the improvement needed appears to be developing a method to formulate the aerodynamic matrices that have the same d.o.f. as the plate finite elements and to include a sufficient number of aerodynamic boxes in each finite element.

In this study, the three-dimensional flow theory is used in the development of a direct finite-element procedure for panel flutter analysis. The aerodynamic matrix is derived by using the principle of virtual work. The aerodynamic forces or velocity potentials that produce the work are obtained for each d.o.f. by the Mach box method. Each finite element is divided into several boxes. The aerodynamic influence coefficients for each pair of sending and receiving boxes are evaluated, for each d.o.f., by the method of Gaussian quadrature. The velocity potential at each receiving box is obtained, for each d.o.f., by summation of the product of corresponding downwash and influence coefficients for all sending boxes. It should be noted that the box method was used by Cunningham[10] in conjunction with a Galerkin's modal method for panel flutter analysis. Three-dimensional aerodynamic theory was also employed by Dowell and Voss[11] in a theoretical and experimental correlation study of panel flutter.

The 16 d.o.f. conforming rectangular plate element[12] was used for example demonstrations. Flutter boundaries were found for clamped rectangular panels with various aspect ratios. The thickness ratios required to prevent an aluminum panel from flutter at sea level were plotted for Mach numbers ranging from 1.05 to 3. Results were found in good agreement with Cunningham's[10] solution.

The initial in-plane tensile stresses were then included for finding the flutter boundaries for a clamped square aluminum panel. The thickness ratios required to prevent the panel from flutter at 25,000-ft altitude were obtained for Mach numbers ranging from 1.05 to 2 for various values of the tension parameter. It was found that the critical flutter mode changed abruptly as Mach number was varied.

Equations of Motion

The free vibration equations of motion for a finite-element panel subjected to the effect of stiffness, in-plane force, inertia, and aerodynamic pressure may be written as

$$[k]\{q\}+[N]\{q\}+[M]\{\ddot{q}\}+[A]\{q\}=\{0\} \tag{1}$$

where $[K]$, $[N]$, $[M]$, and $[A]$ are, respectively, the stiffness, incremental stiffness, mass, and aerodynamic matrices assembled for the whole finite-element system. The vector $\{q\}$ contains the nodal degrees of freedom for the whole panel system. In this section, only the system aerodynamic matrix is formulated.

A. Principle of Virtual Work

For a system of plate finite elements, the deflection and aerodynamic pressure may be written by separating the time and space variables as, respectively,

$$\bar{z}(x,y,t)=z(x,y)e^{i\omega t} \tag{2a}$$

$$\bar{p}(x,y,t)=p(x,y)e^{i\omega t} \tag{2b}$$

where the coordinates are defined in Fig. 1.

The strain energy for the panel system is equal to the work produced by the aerodynamic pressure

$$U=\tfrac{1}{2}\iint z(x,y)p(x,y)\,dx\,dy \tag{3}$$

The deflection function for the total finite-element system may be assumed as

$$z(x,y)=\sum_{j=1}^{N} f_j(x,y)q_j=\{f\}^T\{q\} \tag{4}$$

where $f_j(x,y)$ represents the assembled shape function corresponding to the nodal d.o.f. q_j and N is the number of degrees of freedom for the whole panel system.

Similarly, the aerodynamic pressure may be assumed as

$$p(x,y)=\sum_{j=1}^{N} P_j(x,y)q_j=\{P\}^T\{q\} \tag{5}$$

where $P_j(x,y)$ is defined as the pressure function associated with the shape function $f_j(x,y)$ and d.o.f. q_j.

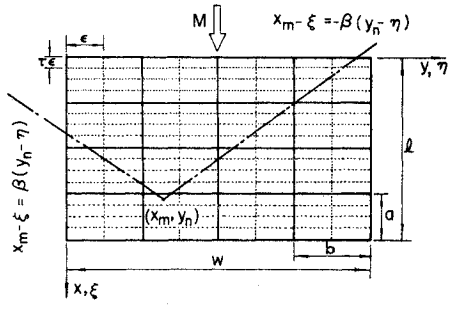

Fig. 1 Panel divided into finite elements (solid lines) and boxes (dash lines) with coordinates, dimensions, and Mach cone.

Substituting Eqs. (4) and (5) into Eq. (3), the strain energy expression becomes

$$U=\tfrac{1}{2}\{q\}^T[A]\{q\} \tag{6}$$

with

$$[A]=\iint\{f\}\{P\}^T dx\,dy \tag{7}$$

Using the principle of virtual work, Eq. (7) yields the aerodynamic matrix as defined in Eq. (1).

B. Aerodynamic Matrix and Aerodynamic Pressure

The aerodynamic perturbation pressure is obtained from the linearized three-dimensional supersonic unsteady potential flow theory. When associated with the d.o.f. q_j and the shape function $f_j(x,y)$, the perturbation pressure may be expressed in terms of the velocity potential through the relation (see, for example, Ref. 13),

$$p_j(\bar{x},\bar{y})=-\frac{\rho V}{\ell}\left(\frac{\partial\phi_j}{\partial\bar{x}}+i\frac{\omega\ell}{V}\phi_j\right) \tag{8}$$

where ϕ_j is the velocity potential associated with d.o.f. q_j.

The coefficient at the ith row and jth column of the aerodynamic matrix $[A]$ is obtained by substituting Eq. (8) into Eq. (7),

$$A_{ij}=-\frac{\rho V}{\ell}\int\!\!\int f_i(\bar{x},\bar{y})\left(\frac{\partial\phi_j}{\partial\bar{x}}+i\frac{\omega\ell}{V}\phi_j\right)d(\ell\bar{x})\,d(w\bar{y}) \tag{9}$$

Performing integration by parts and assuming restrained trailing edge, Eq. (9) becomes

$$A_{ij}=\frac{\rho V}{\ell}\int\!\!\int\phi_j\left(\frac{\partial f_i}{\partial\bar{x}}-i\frac{\omega\ell}{V}f_i\right)d(\ell\bar{x})\,d(w\bar{y}) \tag{10}$$

where the quantity within the first parentheses is the complex conjugate of the downwash ratio for unit d.o.f. q_i and unit panel length. The coefficient A_{ij} is evaluated numerically through the following simple summation

$$A_{ij}=\frac{\rho V}{\ell}\sum\phi_j\left(\frac{\partial f_i}{\partial\bar{x}}-i\frac{\omega\ell}{V}f_i\right)\cdot(\text{Box Area}) \tag{11}$$

where the summation is to be made for every box, and the quantities related to ϕ_j and f_i are evaluated numerically at the center of each box. The method for numerically evaluating the velocity potential at the center of each box is given as follows.

C. Velocity Potential and Aerodynamic Influence Coefficient

The Mach box method as employed by Cunningham[10] is used here to derive the aerodynamic influence coefficients between each pair of boxes and the resulting velocity potential at each box. In this method, each finite element is divided into several equal-size boxes as shown in Fig. 1. The numbers of boxes in the stream and cross-stream directions are defined as B_x and B_{xs}, respectively. The width and length of each box are defined as ϵ and $\tau\epsilon$, respectively, where $\epsilon=w/B_{xs}$ and $\tau=\ell B_{xs}/wB_x$. The boxes are numbered in sequence from the origin with m (or λ) and n (or ν) as the box number in the stream and the cross-stream directions, respectively. The numbers (m,n) and (λ,ν) refer to the receiving and sending boxes, respectively. The boxes are assumed sufficiently small so that the downwash over any sending box is considered as uniformly distributed at any instant, and the resulting perturbation pressure at the center of each receiving box represents the average of the pressure distributed over the box.

The velocity potential at the center of a receiving box (m,n) due to a uniformly distributed but otherwise unspecified downwash $w(\lambda,\nu)$ over the sending box (λ,ν) can be expressed, for harmonic motion, as

$$\bar{\phi}(m,n)=\epsilon w(\lambda,\nu)\alpha_\phi(r,s) \tag{12}$$

where the relative locations in stream and cross-stream directions between the two boxes are defined as $r=m-\lambda$ and $s=n-\nu$, respectively. The aerodynamic influence coefficient is, from Ref. 10,

$$\alpha_\phi(r,s)=\frac{1}{2\pi}\int_{u_1}^{u_2}e^{-i(\beta\bar{\Omega}/2)u}\left\{\cos^{-1}\frac{v_1}{u}-\cos^{-1}\frac{v_2}{u}+\int_{v_1}^{v_2}\frac{\cos[(\beta\bar{\Omega}/2M)(u^2-v^2)^{1/2}]-1}{(u^2-v^2)^{1/2}}dv\right\}du \tag{13}$$

where all the parameters are defined in the Nomenclature.

In Eq. (13), the surface integration limits u_1, u_2, v_1, and v_2 result in only three different forms I_{G1}, I_{G2}, and I_{G3} as shown in Fig. 2.

The first form is for any portion of a sending box λ,ν cut by both sides of the Mach cone so that $v_2=-v_1=u$, and $s=0$:

$$I_{G1}=\frac{1}{2}\int_{u_1}^{u_2}e^{-i(\beta\bar{\Omega}/2)u}J_0\left(\frac{\beta\bar{\Omega}}{2M}u\right)du \tag{14}$$

where J_0 is the Bessel function of the first kind of order zero.

The second form is for portions of a box cut by one side of the Mach cone so that the limits $v_2=u$ and $v_1=2s-1\geq 1$:

$$I_{G2}=\frac{1}{2\pi}\int_{u_1}^{u_2}e^{-i(\beta\bar{\Omega}/2)u}\left\{\cos^{-1}\frac{v_1}{u}+\int_{v_1}^{u}\frac{\cos[(\beta\bar{\Omega}/2M)(u^2-v^2)^{1/2}]-1}{(u^2-v^2)^{1/2}}dv\right\}du \tag{15}$$

The third form is for boxes that are completely within the Mach cone and also for portions of boxes ahead of the point where the Mach line cuts the side of the box:

$$I_{G3}=\frac{1}{2\pi}\int_{u_1}^{u_2}e^{-i(\beta\bar{\Omega}/2)u}\left\{\cos^{-1}\frac{v_1}{u}-\cos^{-1}\frac{v_2}{u}+\int_{v_1}^{v_2}\frac{\cos[(\beta\bar{\Omega}/2M)(u^2-v^2)^{1/2}]-1}{(u^2-v^2)^{1/2}}dv\right\}du \tag{16}$$

The complete $\alpha_\phi(r,s)$ for any one sending box (λ,ν) consists of I_{G1}, I_{G2}, or I_{G3}, or a combination of I_{G1} and I_{G3}, or of I_{G2} and I_{G3}. The types of integrals and limits of integration for computing $\alpha_\phi(r,s)$ for all possible relative locations of box λ, ν and the Mach cone from m, n are given in Ref. 10.

The evaluation of the preceding three integrals is carried out through the method of Gaussian quadrature. In the subsequent numerical examples, three Gaussian points are used in both x and y directions for computing I_{G3}. Five Gaussian points in both x and y directions are used for computing I_{G1} and I_{G2}.

Once all possible values of the aerodynamic influence coefficient $\alpha_\phi(r,s)$ are obtained for a certain shape function $f_j(\bar{x},\bar{y})$, the total velocity potential at the center of a receiving box (m,n) for the downwash associated with the same shape function is a weighted sum of the $\bar{\phi}_j(m,n)$ defined in Eq. (12):

$$\phi_j(m,n)=V\epsilon\sum_{\lambda}\sum_{\nu}\frac{w_j(\lambda,\nu)}{V}\alpha_\phi(r,s) \tag{17}$$

The summation is extended over all the sending boxes. The downwash ratios $w_j(\lambda,\nu)/V$ for a unit d.o.f. q_j are the total

time derivatives of the shape function $f_j(\bar{x},\bar{y})e^{i\omega t}$,

$$\frac{w_j}{V}=\frac{1}{\ell}\left(\frac{\partial f_j}{\partial \bar{x}}+i\frac{\omega\ell}{V}f_j\right) \tag{18}$$

Once the velocity potentials are obtained for each box for each shape function, they can readily be substituted into Eq. (11) for computing the aerodynamic matrix for the whole panel system.

Formulation for Flutter Determinant

One of the crucial steps in the finite-element flutter formulation is the grouping of parameters and nondimensionalization so that the solution is general enough to include every parameter. The equations of motion (1) are rewritten, in an element form, as

$$\left\{\Omega\left[c_1[k]+Fc_2[n]\right]-\left[c_3[m]-c_4[A]\right]\right\}\{q\}=\{0\} \tag{19}$$

where $\Omega=\omega_1^2/\omega^2(1+ig)$ is the flutter eigenvalue parameter, and

$$c_1=\frac{\mu(\ell/a)^5D}{\omega_1^2\sigma h\ell^4}\;;\; c_2=\mu(\ell/a)^3 \tag{20a}$$

$$c_3=\mu(\ell/a)\qquad ;\; c_4=\left(\frac{\ell}{a}\right)^3\left(\frac{\epsilon}{\ell}\right)\left(\frac{1}{k_\ell}\right)^2\left(\frac{\tau\epsilon^2}{ab}\right) \tag{20b}$$

The element matrix terms are obtained as

$$k_{ij}=\int_0^1\int_0^1\left[\frac{\partial^2 f_i}{\partial\bar{x}^2}\frac{\partial^2 f_j}{\partial\bar{x}^2}+\left(\frac{a}{b}\right)^4\frac{\partial^2 f_i}{\partial\bar{y}^2}\frac{\partial^2 f_j}{\partial\bar{y}^2}+\nu\left(\frac{a}{b}\right)^2\frac{\partial^2 f_i}{\partial\bar{x}^2}\frac{\partial^2 f_j}{\partial\bar{y}^2}+\nu\left(\frac{a}{b}\right)^2\frac{\partial^2 f_j}{\partial\bar{x}^2}\frac{\partial^2 f_i}{\partial\bar{y}^2}+2(1-\nu)\left(\frac{a}{b}\right)^2\frac{\partial^2 f_i}{\partial\bar{x}\partial\bar{y}}\frac{\partial^2 f_j}{\partial\bar{x}\partial\bar{y}}\right]d\bar{x}d\bar{y} \tag{21}$$

$$n_{ij}=\int_0^1\int_0^1\left[\frac{\partial f_i}{\partial\bar{x}}\frac{\partial f_j}{\partial\bar{x}}+\frac{N_y}{N_x}\frac{\partial f_i}{\partial\bar{y}}\frac{\partial f_j}{\partial\bar{y}}+\frac{N_{xy}}{N_x}\frac{\partial f_i}{\partial\bar{x}}\frac{\partial f_j}{\partial\bar{y}}+\frac{N_{xy}}{N_x}\frac{\partial f_j}{\partial\bar{x}}\frac{\partial f_i}{\partial\bar{y}}\right]d\bar{x}d\bar{y} \tag{22}$$

$$m_{ij}=\int_0^1\int_0^1 f_i f_j\,d\bar{x}d\bar{y} \tag{23}$$

$$A_{ij}=\sum\frac{\phi_j}{V\epsilon}\left(\frac{\partial f_i}{\partial\bar{x}}-i\frac{\omega a}{V}f_i\right) \tag{24}$$

The shape functions $f(\bar{x},\bar{y})$ are nondimensional. For Eq. (24), the shape functions are assembled ones. It is important to note that Eqs. (19-24) are suitable for any plate finite element as long as it is a displacement model.

Equation (19) constitutes an eigenvalue problem. The flutter solution is obtained by first assuming a value of reduced frequency k_ℓ, then varying the mass ratio $1/\mu$ incrementally and solving for the corresponding eigenvalues Ω. When the structural damping coefficient g changes from negative to positive, the panel goes from the stable region to unstable region, and vice versa.

Results

The 16 d.o.f. conforming rectangular plate finite element[12] was employed to demonstrate the present formulation and procedure. The examples chosen were rectangular panels, stressed as well as unstressed, with clamped edges. For the unstressed panels, a solution by Cunningham[10] using the box method (400 boxes) and Galerkin's modal approach (6 to 16 modes) were available for comparison.

In all of the examples studied here, the flutter mode shapes were assumed symmetrical about the center chord-line of the panel. Thus, only half of each panel was modeled by finite elements. In all cases, two elements in the cross-stream direction were used for half of the panel. The number of elements in the stream direction varied from 4 to 10, dependent on the dominating flutter mode numbers. Each element was divided into 4 by 2 boxes in the stream and cross-stream directions, respectively.

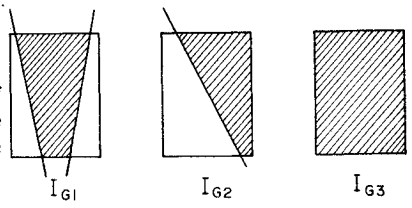

Fig. 2 Three forms of integrals for computing the aerodynamic influence coefficients.

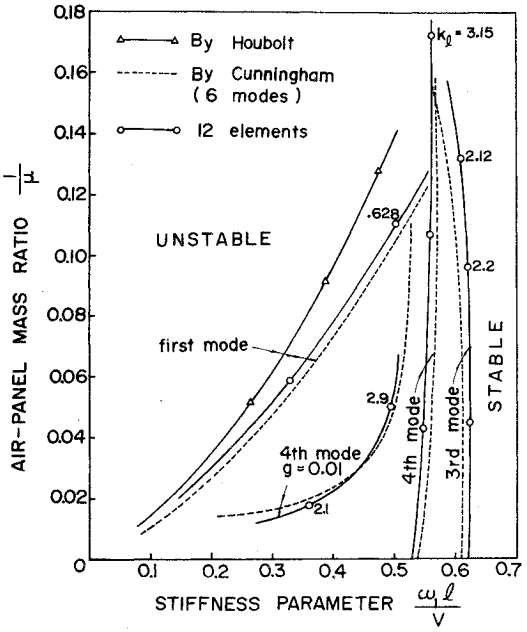

Fig. 3 Flutter boundaries for clamped panel with $\ell/w=1$ and $M=1.3$.

It is important to note that symmetry does not exist for the mesh of boxes unless the Mach cone apex lies in the center chord-line of the panel. The boxes on the other (disregarded) half of the panel can, however, still be accounted for since their deflection shapes are known by symmetry.

Case 1: Clamped Panels with Various Chord-Span Ratio at $M=1.3$

The rectangular panels with all edges clamped and chord-span ratios (ℓ/w) equal to 0, ¼, ½, 1, 2, and 4 were studied for the case $M=1.3$. The results for flutter boundaries for panel with $\ell/w=1$ are shown in Fig. 3. Good agreement with Cunningham's results is seen. The first mode flutter boundary obtained by Houbolt[14] using the piston theory is also shown. The results for panels with other aspect ratios are presented in Ref. 15 with similar level of agreement with those obtained by Cunningham. The corresponding mode shapes are also given in Ref. 15.

Case 2: Clamped Panel with $\ell/w=2$ at Various Mach Numbers

A clamped panel with $\ell/w=2$ and under airstream with various Mach numbers was studied. One of the main purposes was to establish a curve for the thickness ratios required to prevent the panel from flutter at various airspeeds.

The first mode flutter boundaries for panel with $\ell/w=2$ and $M=1.05$, 1.1, 1.4, 1.5, 2, and 3 are first obtained.[15] Corresponding to each curve, one can construct a parabola for the equation that $xy=C$ or $(\rho\ell/\sigma h)(\omega_1\ell/V)=C$. The constant C is dependent on the densities of the air and

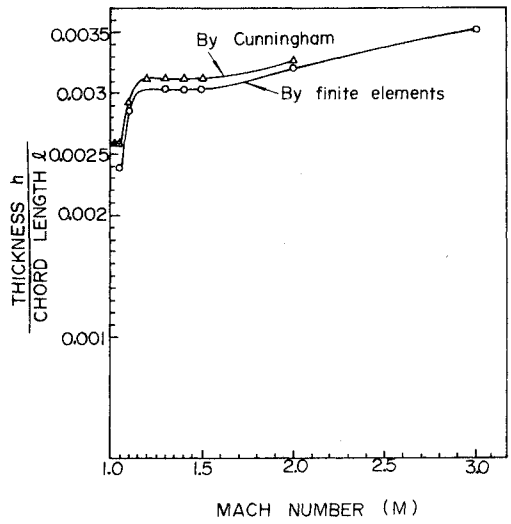

Fig. 4 Thickness ratios required to prevent flutter for clamped aluminum panel with $\ell/w = 2$ at sea level.

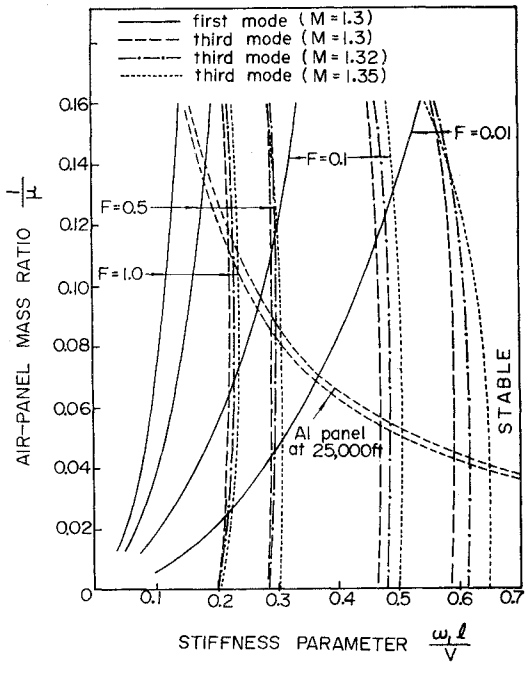

Fig. 5 Flutter boundaries for clamped square panel with $M = 1.3$, 1.32, 1.35, and various tension parameters.

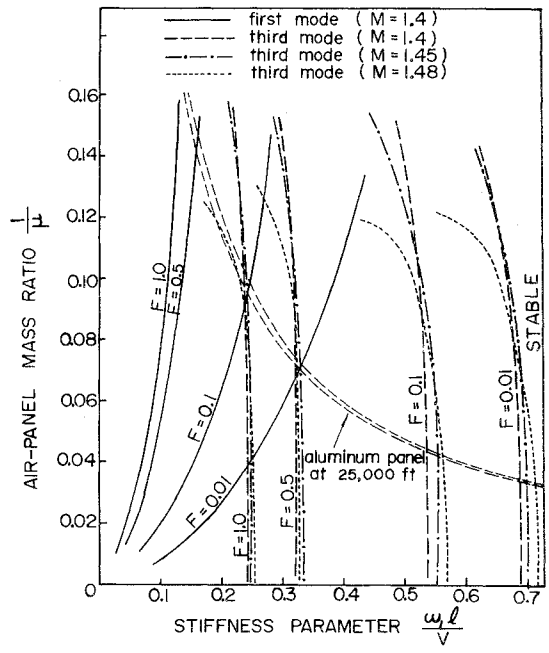

Fig. 6 Flutter boundaries for clamped square panel with $M = 1.4$, 1.45, 1.48, and various tension parameters.

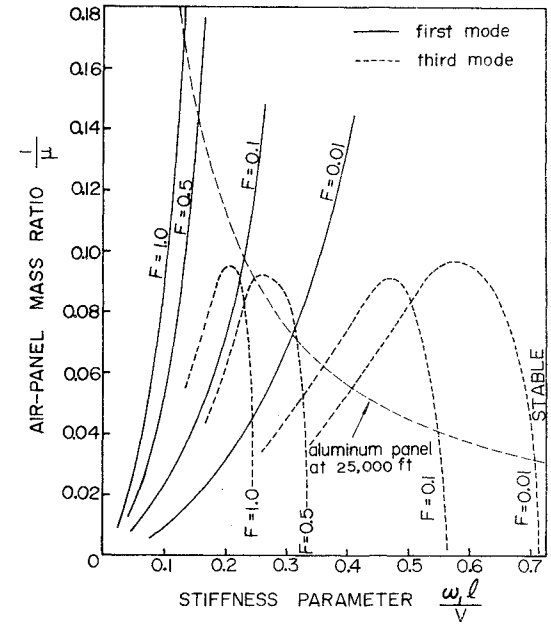

Fig. 7 Flutter boundaries for clamped square panel with $M = 1.5$ and various tension parameters.

aluminum, the dimensions of the panel, the airspeed, and the bending rigidity of the panel. The intersecting point between a pair of parabola and flutter curve gives the thickness ratio h/ℓ required to prevent the aluminum panel from flutter at sea level. For all Mach numbers considered, the first mode flutter boundaries are critical for sea-level altitude. The results are shown in Fig. 4. The present results are slightly on the unconservative side as compared to the results of Cunningham.

Case 3: Clamped Square Panels with Various Tension Parameters and Mach Numbers

One of the advantages of the finite-element method is that the effect of in-plane forces can be included in a direct and accurate fashion. To demonstrate this, a square clamped panel was chosen, and four different tension parameters, $F = 0.01$, 0.1, 0.5, and 1 were considered. The flutter boundaries were obtained for various Mach numbers and shown in Figs. 5-8.

Figure 5 shows that for $M = 1.3$, 1.32, 1.35, and various tension parameters, the third mode boundaries are the critical flutter boundaries. Results for $M = 1.1$ and 1.2 are available in Ref. 15. For $M = 1.2$, the first mode flutter boundaries dominate the high mass ratio region, and the third mode flutter boundaries dominate the low mass ratio region.

Figure 6 shows the flutter boundaries for $M = 1.4$, 1.45, 1.48 and various tension parameters. The third mode flutter boundaries shift to the right as the Mach number increases. It is interesting to see that the top portion of the third mode flutter boundaries begin to bend down to the left as the Mach number increases.

Figure 7 shows that for $M = 1.5$ and various tension parameters, the third mode flutter boundaries continue to bend down rapidly with a slight increase in Mach number. Figure 8 shows that for $M = 1.54$ and various tension

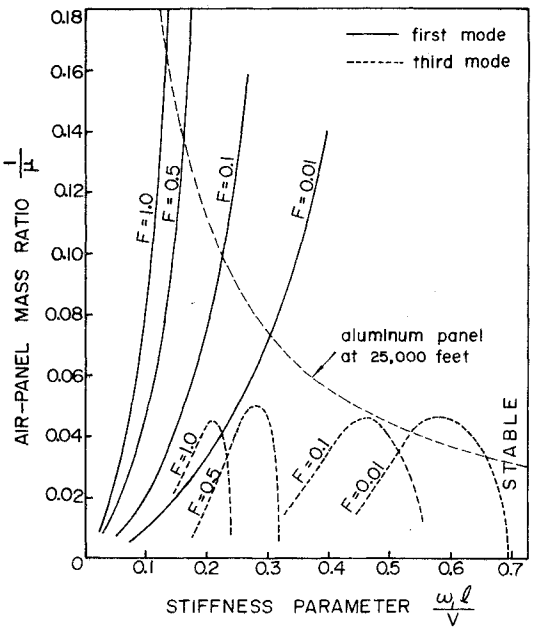

Fig. 8 Flutter boundaries for clamped square panel with $M = 1.54$ and various tension parameters.

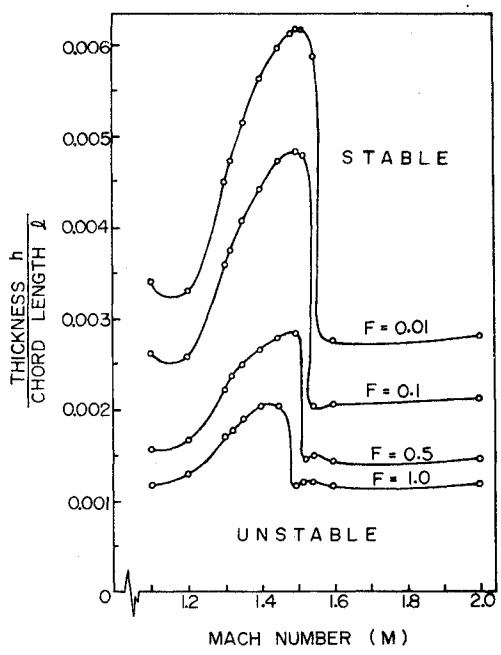

Fig. 9 Thickness ratios required to prevent flutter for a square clamped aluminum panel at 25,000 ft above sea level under different tension parameters.

parameters, the third mode flutter boundaries bend down substantially to be small loops. They only dominate the lower range of the mass ratio.

Results for $M = 1.6$ and 2.0 are available in Ref. 15. In the two cases, the third mode flutter boundaries disappear and the first mode boundaries again dominate the whole mass ratio region.

The dashed parabolas for aluminum panel at 25,000 ft above sea level are shown in Figs. 5-8 for all Mach numbers considered. By collecting all the intersecting points between the dashed parabolas and the critical flutter boundaries, the results for thickness ratios required to prevent the panel from flutter are shown in Fig. 9 for various Mach numbers and tension parameters. There are some extra data points in Fig. 9 which are not obtained from Figs. 5-8. They are referred to Ref. 15. The plots of flutter mode shapes are also referred to Ref. 15.

In Fig. 9, the critical flutter boundaries were dominated by the third mode in the Mach region between approximately 1.2 and 1.5. For other lower and higher Mach regions, the first mode flutter boundaries dominate. The sharp drops in the curves are due to the abrupt changes in critical flutter modes. The beneficial effect of introducing in-plane tensions to reduce the required panel thickness to avoid flutter is clearly demonstrated.

Concluding Remarks

A basic finite-element procedure for panel flutter analysis has been developed and numerical examples presented. The following concluding remarks may be made.

1) The three-dimensional supersonic unsteady potential flow theory was employed. This theory allows the treatment of panels with finite aspect ratio. It is particularly advantageous at low supersonic range ($1 < M < \sqrt{2}$) for panels with chord-span ratio less than one, where the piston theory does not give satisfactory results.[14]

2) The finite-element method offers a set of elegant and straightforward eigenvalue equations. It can be used directly to solve for flutter frequencies and mode shapes without having to find the natural frequencies and modes as well as the number of modes to be used before the eigensolution, and also without requiring the computation of mode shapes after the eigensolution. Of course, one must investigate the convergence of the finite-element solution itself.

3) If the modal method is used in panel flutter analysis, one could use the natural frequencies and modes found by the finite-element method. Such a procedure is, however, basically different from the present finite-element method. It is the one commonly employed in lifting-surface flutter analysis, of course.

4) The formulations here [Eqs. (19-24)] are general. They are readily applicable to any plate finite-element displacement model whose shape functions are known.

5) Figures 3 and 4 show that the present results agree well with the Galerkin's modal solution by Cunningham.

6) Figures 5-9 show that the critical flutter modes for a square clamped panel change abruptly as the Mach number is varied.

7) Figure 9 clearly demonstrates the beneficial effect of in-plane tensions.

8) The present results may provide useful data to the flutter analysts and designers.

In order to attain the present state-of-the-art of panel flutter, this development should be extended to include the effects of pressure differential and buckling and shear layer aerodynamics. Such effects were considered in Refs. 16-19.

Acknowledgment

This work is partially supported by the Air Force Flight Dynamics Lab. under Job Order 23070501. Preliminary results of this paper were presented in the 2nd International Symposium on Finite-Element Method in Flow Problems, Rappalo, Italy, June 14-18, 1976.

References

[1] Dowell, E.H., *Aeroelasticity of Plates and Shells,* Noordhoff International Publishing, Leyden, The Netherlands, 1975.

[2] *Aerodynamic Flutter,* AIAA Selected Reprint Series, Vol. V, edited by I.E. Garrick, New York, 1969.

[3] Olson, M.D., "Finite Elements Applied to Panel Flutter," *AIAA Journal,* Vol. 5, Dec. 1967, pp. 2267-2270.

[4] Olson, M.D., "Some Flutter Solutions Using Finite Elements," *AIAA Journal,* Vol. 8, April 1970, pp. 747-752.

[5] Appa, K. and Somashekar, B.R., "Application of Matrix Displacement Methods in the Study of Panel Flutter," *AIAA Journal,* Vol. 7, Jan. 1969, pp. 50-53.

[6] Appa, K., Somashekar, B.R., and Shah, C.G., "Discrete Element Approach to Flutter of Skew Panels with In-Plane Forces under

Yawed Supersonic Flow," *AIAA Journal*, Vol. 8, Nov. 1970, pp. 2017-2022.

[7] Sander, G., Bon, C., and Geradin, M., "Finite Element Analysis of Supersonic Panel Flutter," *International Journal for Numerical Methods in Engineering*, Vol. 7, Nov. 1973, pp. 379-394.

[8] Yang, T.Y., "Flutter of Flat Finite-Element Panels in a Supersonic Potential Flow," *AIAA Journal*, Vol. 13, Nov. 1975, pp. 1502-1507.

[9] Appa, K., "Kinematically Consistent Unsteady Aerodynamic Coefficients in Supersonic Flow," *International Journal for Numerical Methods in Engineering*, Vol. 2, Oct. 1970, pp. 495-507.

[10] Cunningham, H.J., "Flutter Analysis of Flat Rectangular Panels Based on Three-Dimensional Supersonic Unsteady Potential Flow," NASA TR R-256, 1967.

[11] Dowell, E.H. and Voss, H.M., "Theoretical and Experimental Panel Flutter Studies in the Mach Number Range 1.0 to 5.0," *AIAA Journal*, Vol. 3, Dec. 1965, pp. 2292-2304.

[12] Bogner, F.K., Fox, R.L., and Schmit, L.A., "The Generation of Interelement-Compatible Stiffness and Mass Matrices by the use of Interpolation Formulas," *Proceedings of the Conference on Matrix Methods in Structural Mechanics*, Air Force Flight Dynamics Lab, TR-66-80, 1966, pp. 397-443.

[13] Watkins, C.E., "Three Dimensional Supersonic Theory," *AGARD Manual on Aeroelasticity*, Nov. 1960, Part II, Chap. 5.

[14] Houbolt, J.C., "A Study of Several Aerothermoelastic Problems of Aircraft Structures in High-Speed Flight," Doctor of T.S. Thesis, The Swiss Federal Institute of Technology, Leeman, Zürich, 1958.

[15] Sung, S.H., "Finite-Element Flutter Analysis of Flat Panels in 3-D Supersonic Unsteady Potential Flow," Ph.D. Thesis, School of Aeronautics and Astronautics, Purdue University, W. Lafayette, Ind.; Dec. 1976.

[16] Ventres, C.S. and Dowel, E.H., "Comparison of Theory and Experiment for Nonlinear Flutter of Loaded Plates," *AIAA Journal*, Vol. 8, Nov. 1970, pp. 2022-2030.

[17] Ventres, C.S. and Kang, C.K., "Large Amplitude Flutter of a Low Aspect Ratio Panel at Low Supersonic Speeds – Comparison of Theory and Experiment," Princeton University AMS Rept. No. 1116, Aug. 1973.

[18] Dowell, E.H., "Generalized Aerodynamic Forces on a Plate Undergoing Transient Motion in a Shear Flow with an Application to Panel Flutter," *AIAA Journal*, Vol. 9, May 1971, pp. 834-841.

[19] Dowell, E.H., "Aerodynamic Boundary-Layer Effects on Flutter and Damping of Plates," *Journal of Aircraft*, Vol. 10, Dec. 1973, pp. 734-738.